

Improving the physical and mechanical characteristics of unalloyed titanium VT1-0 and studying the effect of selective laser melting parameters

© M.Yu. Gryaznov, S.V. Shotin, V.N. Chuvildeev, A.N. Sysoev, N.V. Melekhin, A.V. Piskunov, N.V. Sakharov, A.V. Semenycheva, A.A. Murashov

Lobachevsky University of Nizhny Novgorod,
603022 Nizhny Novgorod, Russia
e-mail: gryaznov@nifti.unn.ru

Received August 25, 2022

Revised October 24, 2022

Accepted October 25, 2022

Comprehensive studies of the physical and mechanical properties and structure of VT1-0 titanium samples processed by selective laser melting have been carried out. High strength characteristics (the ultimate tensile strength of 820 MPa, the yield strength of 710 MPa) have been achieved. These exceed by 2 times the values for this material produced using conventional technology. The formation of the martensitic α' -phase, obtained due to the high crystallization rates realized in selective laser melting process, is the reason for the increase in the mechanical characteristics of titanium VT1-0. Mechanical characteristics of titanium VT1-0 subjected to high-temperature annealing demonstrated a monotonous decrease in strength parameters by 15% and an increase in plastic characteristics by 30%. It is shown that the technology of selective laser melting makes it possible to solve the problem of improving the strength characteristics of unalloyed titanium to create a new class of medical devices.

Keywords: unalloyed titanium, VT1-0, additive technology, selective laser melting, density, strength, plasticity, elastic modulus, microstructure, implants for surgery.

DOI: 10.21883/TP.2023.02.55477.209-22

Introduction

Titanium alloys are used in many biomedical applications, such as orthopedic and dental implants, artificial joints, bone plates, cardiostimulator housings, valve prostheses, etc. [1]. The widespread use of these materials is associated with high values of strength, fracture toughness and fatigue endurance [2]. Besides, a stable and bioinert oxide layer is spontaneously formed on the surface of titanium products, and therefore titanium has a high corrosion resistance and a low tendency to ions formation in aqueous media [3]. Currently, one of the metal materials most in demand in medicine is the titanium alloy of the system Ti–6%Al–4%V [4,5], which is used for the production of implants and endoprostheses. At the same time, the paper [6] shows that the presence of vanadium and aluminum in this alloy over time can have a negative complex effect on the health of patients. Unalloyed titanium has no this disadvantage, but the main obstacle to its use as material for endoprostheses and implants is its low mechanical properties [4]. Improving the mechanical characteristics of unalloyed titanium is an important objective, since this will significantly expand the scope of its application.

In recent years, an important vector for the materials science development for medicine was researches and developments aimed at creating personalized medical devices for osseointegration, taking into account the anatomical and physiological characteristics of each patient [7,8]. In some

cases the modern medical protocols allow the use of not typical osseointegrated products, but personalized endoprostheses and implants made according to CAD-models obtained from the results of X-ray study, computed tomography and 3D-reconstruction [9].

Thus, it can be stated that there are two important objective in modern medical materials science: the creation of a technology for improving the mechanical characteristics of materials based on unalloyed titanium, and the creation of a technology for obtaining products of complex geometry (including endoprostheses and implants) necessary for the development of the direction related to personalized medical devices use. To solve these tasks the selective laser melting (SLM) technology can be used, i.e. actively developing additive 3D-printing technology, which makes it possible to create precision products of complex shape [10–12]. Despite a large number of studies aimed at improving the mechanical characteristics of SLM-titanium [13–20], the task of a significant increase in the strength of unalloyed titanium was not yet solved and remains very relevant.

In this paper, samples of unalloyed titanium VT1-0 were created by the SLM method, they are twice as strong compared to titanium samples obtained by traditional metallurgical methods. The paper relates to the study of the physical and mechanical properties and structure of titanium VT1-0 and the study of the SLM parameters influence on them.

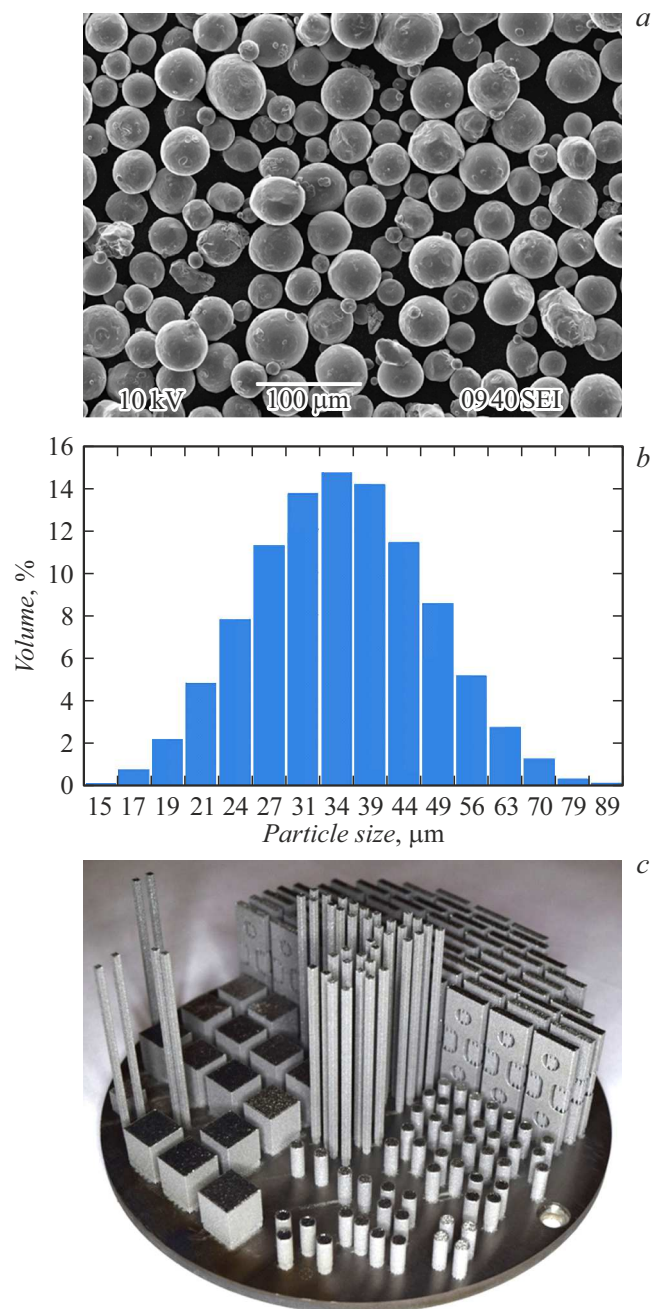


Figure 1. SEM image of particles (a); histogram of particles distribution by sizes for titanium powder VT1-0 (b); samples for study made by the SLM (c).

1. Method of obtaining and study the material

The objects of study are samples of unalloyed titanium VT1-0 (hereinafter „SLM-titanium VT1-0“), manufactured using the SLM technology on a modernized unit MTT Realizer SLM100 using domestic powder produced by LLC „NORMIN“. Chemical composition of the powder according to the manufacturer's certificate (wt.%): Fe —

0.14, O — 0.16, Si — 0.01, C — 0.021, N — 0.03, H — 0.006, Ti — base. Powder particles with an average size of 35 μm have a spherical shape (Fig. 1, a) and the distribution by sizes shown in Fig. 1, b.

In order to study the influence of the SLM process parameters on the physical and mechanical properties of VT1-0 titanium, several series of samples were prepared using different SLM modes (Fig. 1, c): the laser power (hereinafter „laser power“) varied from 70 to 100 W, the speed of the laser beam (hereinafter „scanning speed“) — from 30 to 500 mm/s. Other parameters of the SLM remained constant during the construction of all samples: the thickness of the powder layer was 70 μm, and the hatch spacings was 120 μm. The temperature of the platform was maintained constant and equal to 220°C. All manipulations with the powder (vibration sieving, drying in a heat chamber, etc.) and the SLM process were carried out in high-purity argon (99.998 wt.%).

The granulometric composition of the powder was studied on a SALD-2300 Shimadzu laser particle size analyzer. The density of cube samples 10 × 10 × 10 mm was measured using the hydrostatic weighing technique on Sartorius CPA225D analytical balance with an error of 0.1% and is presented as a percentage of the theoretical density of titanium (4.51 g/cm³).

Tensile tests were carried out using Tinius Olsen H25K-S unit at room temperature with a constant deformation rate of 0.01 mm/s of cylindrical samples with a working area with a diameter and length equal to 3 and 15 mm, respectively. Structural studies were carried out using Jeol JSM 6490 and Tescan Vega 2 scanning electron microscopes. For metallographic studies the surface of cubic samples 10 × 10 × 10 mm was mechanically polished using diamond pastes and subjected to electrochemical etching. Young's modulus was measured using Agilent NanoIndenter G200 probe system for measuring mechanical parameters by the Berkovich continuous indentation method. The indentation of the central section of cubic samples prepared for metallographic studies was carried out as follows: the distance between the indentations — about 1 mm, the depth of indentation — 0.4–0.8 μm; deformation rate — 0.05 s⁻¹.

2. Results of experimental studies

The results of studies of the SLM process parameters influence on the strength and plastic characteristics of VT1-0 titanium are shown in Fig. 2 as diagrams of the ultimate tensile strength and elongation to failure vs. the laser power P and scanning speed V . As can be seen from Fig. 2, a, the maximum strength of 810–820 MPa is observed at SLM parameters 90–100 W and 100–150 mm/s, the minimum values of the ultimate tensile strength 640–690 MPa were obtained with parameters 70–75 W, 400–500 mm/s. The maximum values of elongation to failure 16–17% were obtained in the range of SLM parameters 90–100 W and 100–150 mm/s (Fig. 2, b), minimum values 5–8% — for

SLM parameters 70–75 W, 400–500 mm/s and 95–100 W, 30–60 mm/s.

Studies of the influence of SLM process parameters on the value of the physical yield strength showed that the values vary in the range from 520 to 710 MPa (Fig. 3, *a*). Maximum values 700–710 MPa are observed at SLM parameters 90–100 W and 100–200 mm/s, minimum values 520 MPa — at 70–75 W, 400–500 mm/s.

The results of studying the elastic properties by the nanoindentation method are shown in Fig. 3, *b*, which shows a diagram of average values of Young’s modulus (averaging each value over 80 indentations) vs. the main SLM parameters. The average values of Young’s modulus for samples obtained under different SLM modes vary from 88 to 110 GPa.

The results of studying the influence of the SLM process parameters on the density of VT1-0 titanium are shown in Fig. 4, *a* as a diagram of the relative density vs. the laser power and scanning speed. It can be seen from the Figure that the maximum values of the relative density 99.8% were obtained using the SLM parameters 90–100 W and 150 mm/s, the minimum values 90–92% — in two ranges

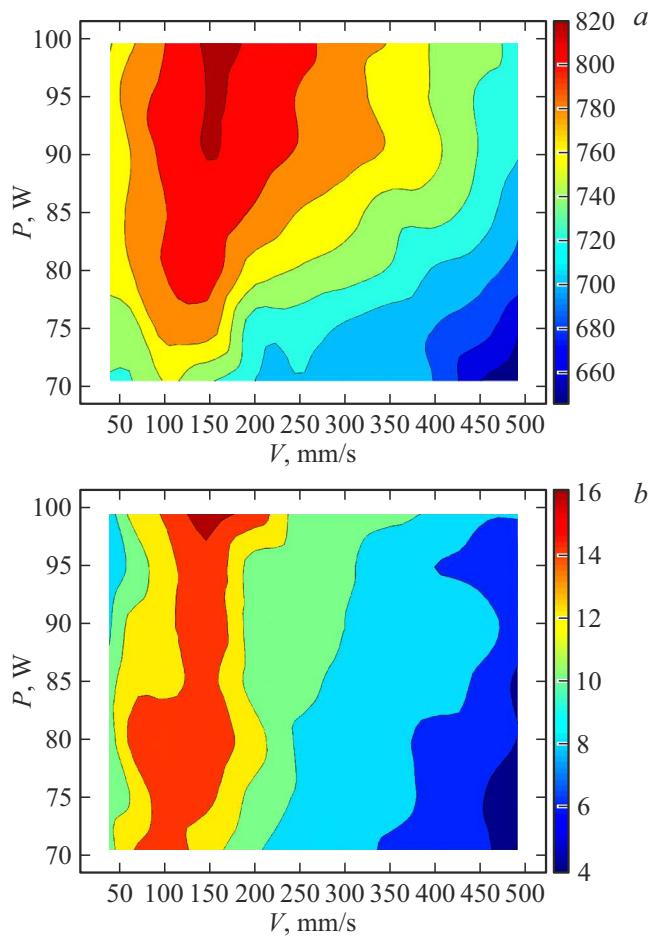


Figure 2. Ultimate tensile strength (*a*) and elongation to failure (*b*) of SLM-titanium VT1-0 vs. laser power P and scanning speed V .

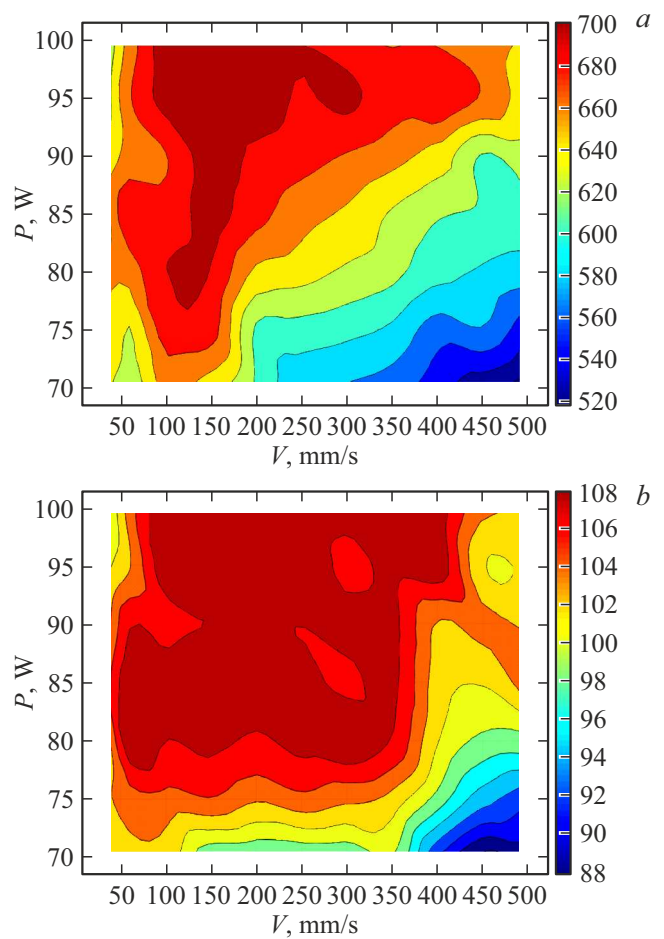


Figure 3. Yield strength (*a*) and Young’s modulus (*b*) of SLM-titanium VT1-0 vs. laser power P and scanning speed V .

of parameters 70–90 W, 350–500 mm/s and 95–100 W, 30–60 mm/s.

In order to study the thermal stability of the mechanical properties of SLM-titanium, the effect of annealing temperature on the ultimate tensile strength and relative elongation to failure of titanium VT1-0 samples obtained under the SLM optimal mode 100 W, 150 mm/s. As can be seen from Fig. 4 *b*, the mechanical characteristics of the material do not change after annealing at temperatures of 100 and 200°C. The annealing for one hour in the temperature range 300–800°C leads to a change in the strength and plastic characteristics: in the range 300–700°C, the ultimate tensile strength decreases from 800 to 620 MPa, a further increase in the annealing temperature to 800°C does not lead to change in the ultimate tensile strength; over the entire annealing temperature range of 300–800°C, the elongation to failure increases from 18 to 22%.

Typical images of the microstructure of SLM-samples of titanium VT1-0 obtained using scanning electron microscopy are shown in Fig. 5. In the SLM process a needle microstructure of the martensitic type is formed with an

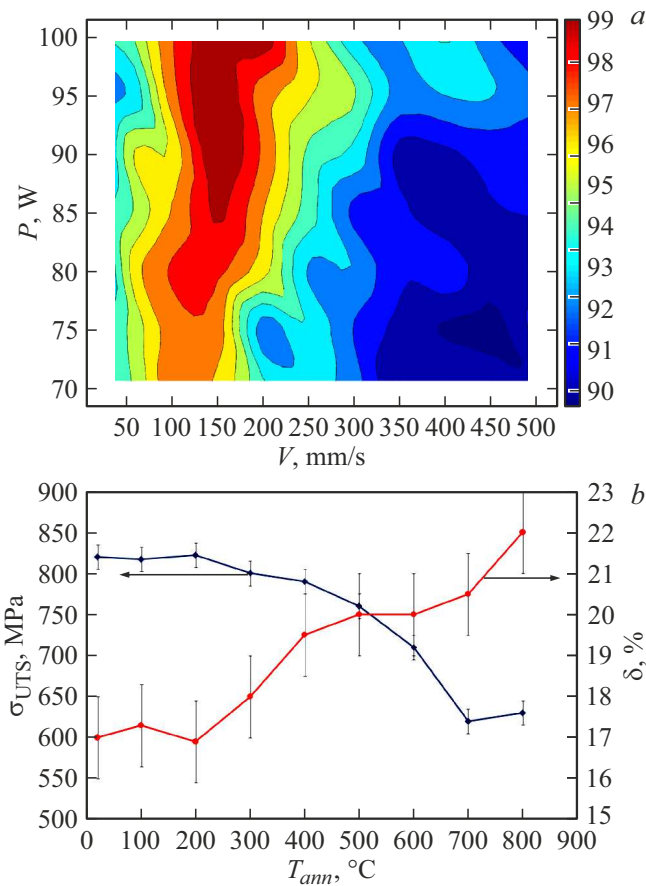


Figure 4. Relative density vs. laser power P and scanning speed V (a), and ultimate tensile strength σ_{UTS} and elongation to failure δ vs. annealing temperature T_{ann} (b) for SLM-titanium VT1-0.

average length of needles $12\ \mu\text{m}$, thickness of $1.5\ \mu\text{m}$, and distance between them of about $1.5\ \mu\text{m}$ (Fig. 5, b). This type of structure is for SLM-titanium [13–19].

As shown in Fig. 5, b, the structure of SLM-titanium after annealing at elevated temperatures is represented by equiaxed polyhedral grains, the martensite phase is not observed. It can be seen that heat treatment at 800°C of SLM-samples leads to the formation of a grain structure with an average grain size of about $20\ \mu\text{m}$.

3. Results and discussion

First of all, the high mechanical characteristics of VT1-0 titanium samples require discussion. As it is known, for titanium VT1-0 obtained by traditional methods the ultimate tensile strength values are $400\text{--}500\ \text{MPa}$ [4]. The high values of ultimate tensile strength ($820\ \text{MPa}$) obtained in this paper can be explained by the presence of a finely dispersed martensitic α' - phase, the occurrence of which is associated with a high crystallization rate of titanium-based materials ($\sim 10^5\text{--}10^7\ \text{K/s}$) [21–23] obtained by SLM methods.

An important result that needs discussion is the obtained dependences of the studied physical and mechanical properties on the SLM parameters. In the first approximation, all dependences obtained can be explained by the influence of the volume fraction of pores arising under nonoptimal SLM modes, which correlates with the material density. To explain the presence of two low-density zones in different areas of the SLM parameters space (Fig. 4, a), it is necessary to introduce the concept of volumetric energy density (VED), which is widely used in papers [13,18–21,24–27] in case of solving the problem of optimizing the parameters of SLM-titanium. The volumetric energy density — is the amount of energy released during SLM per unit of volume

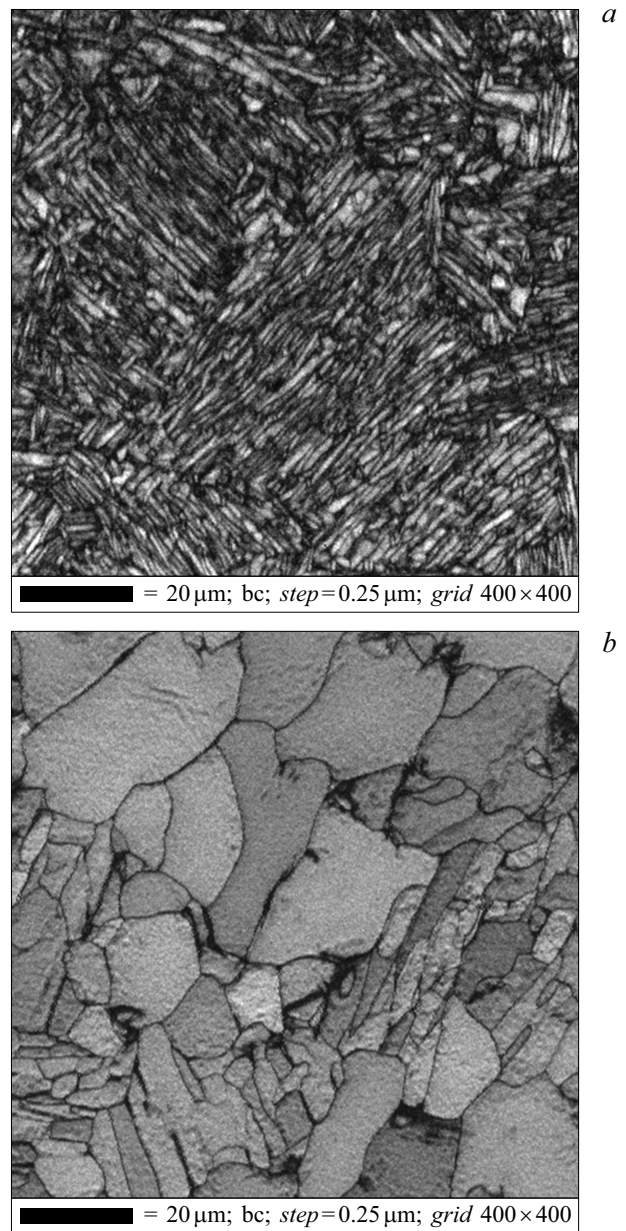


Figure 5. EBSD-quality maps (band contrast) of SLM-titanium VT1-0 samples in the initial state (a) and after annealing at 800°C (b).

SLM process parameters and values of volumetric and linear densities of energy

Parameters	Laser power, P , W	Thickness of layer, h , μm	Scanning speed V , mm/s	Hatch spacing d , μm	Volumetric energy density E_v , J/mm	Linear energy density E_{lin} , J/mm	Reference
CP-Ti (grade 1)	165	100	138	100	120	1.1	[18]
CP-Ti (grade 2)	175	30	800	150	49	0.22	[26]
CP-Ti (grade 3)	50	25	330	80	76	0.15	[20]
CP-Ti (grade 3)	210	30	1000	120	58	0.21	[27]
CP-Ti (grade 3)	90	50	400	50	90	0.23	[21]
BT1-0	100	70	150	120	79	0.66	This study

of material, usually represented by the expression

$$E_v = P/(hdV), \quad (1)$$

where P — laser power, h — layer thickness, d — hatch spacing, V — scanning speed. Note here that the diameter of the focused laser beam should be used as the parameter d . However, many researchers do not have the technical ability to vary the beam diameter (a number of SLM-units have a fixed beam diameter), while the variable parameter is „hatch spacing“, which is used to calculate the specific energy in all the papers mentioned above. On the other hand, since hatch spacing is chosen, as a rule, approximately equal to the beam diameter (with minimal lines overlapping), the difference in the resulted values of the energy density will be insignificant for any choice of the parameter d . In this paper, for the possibility of comparison with the results of other authors, the VED calculation in accordance with expression (1) is carried out using the hatch spacing as d . The Table shows the main SLM parameters and the VED value, which, in accordance with the expression (1) for the optimal mode, was equal to 79 J/mm.

Since in the present paper such SLM parameters as the layer thickness, the distance between the hatch spacings, etc. remained constant, and only the laser power and the scanning speed varied, we introduce the value of the linear energy density (LED), E_{lin} , in the form of a commonly used ratio [24–27]:

$$E_{\text{lin}} = P/V. \quad (2)$$

To estimate the LED effect on the value of relative density, let's convert the diagram shown in Fig. 4, *a* into the plot of density vs. LED shown in Fig. 6, *a*. As can be seen from the Figure, the minimum density values of 90% are observed at the minimum LED values of 0.1–0.2 J/mm. The

obvious reason for the low density under these conditions is the high porosity caused by energy insufficient for uniform melting of the powder at low laser power and high scanning speed. Low relative density values of about 92% are also observed at the highest LED values (3 J/mm), this is due to a combination of processes occurring during SLM in the material if the temperature in the melt pool is close to the evaporation temperature sufficiently long time [28,29]. The crystallization of the melt in the overheated material is performed irregularly, which leads to the formation of numerous small pores in the resulting material [29–31].

A qualitative explanation of the presence of regions with low values of mechanical characteristics on the plane of SLM-parameters „laser power–scanning speed“ can also be given on the basis of plotting their dependence on the LED value. To assess the LED influence on the values of ultimate tensile strength, yield strength, elongation to failure and Young's modulus, we will convert the corresponding diagrams shown in Fig. 1–3 into graphs of the above values versus LED (Fig. 6, *b*). For the convenience of analysis, the data were normalized to the maximum values of the corresponding magnitudes. As can be seen from Fig. 6, *b*, the behavior of all physical and mechanical characteristics has similar non-linear nature: at low LED values (below 0.5 J/mm), low values of the material characteristics under study are observed; the maximum values are achieved in the range of LED values from 0.5 to 0.7 J/mm; at high LED values (above 1 J/mm) a decrease in the values of all characteristics is observed. The reason for the characteristics decreasing in two areas is the high porosity of the material, caused by low LED, insufficient for uniform melting of the powder, and high LED, leading to overheating of the material and heterogeneous crystallization with the pores formation.

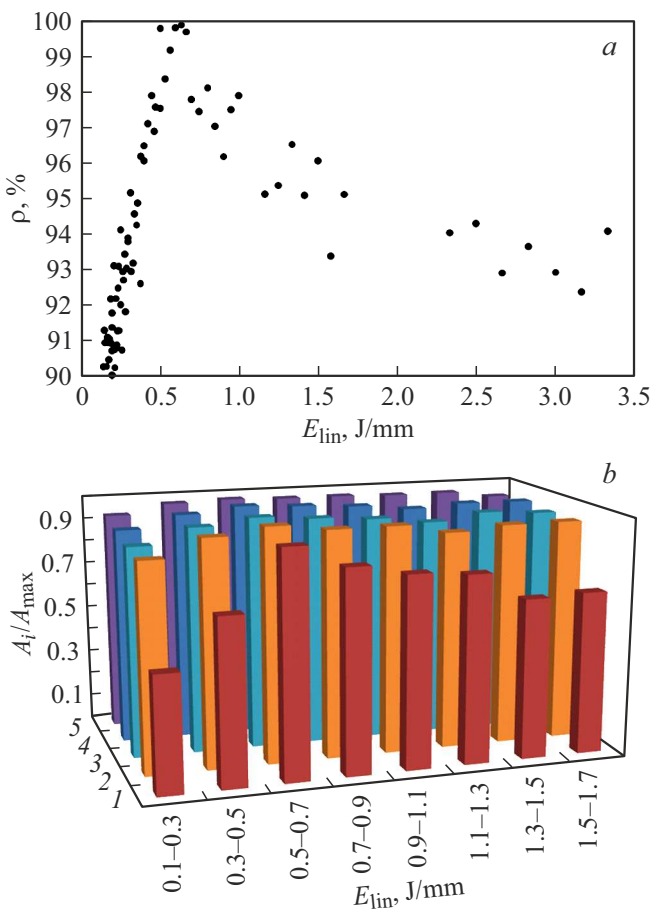


Figure 6. Physical and mechanical characteristics of titanium VT1-0 vs. linear energy density E_{lin} during SLM: *a* — dependence for relative density ρ ; *b* — diagram for normalized values of characteristics A_i/A_{max} : 1 — elongation to failure, 2 — yield strength, 3 — ultimate tensile strength, 4 — relative density, 5 — Young’s modulus.

It can be seen from Fig. 6 that the optimal SLM parameters for obtaining the material with high density (close to theoretical) and high mechanical characteristics are LED values from 0.5 to 0.7 J/mm. At the same time, from the point of view of the prospects for the use of SLM technology for the production of medical devices, the parameters with higher scanning speeds should be recognized as optimal, since this significantly reduces the time of products manufacturing.

The Table contains the values of the volumetric and linear energy obtained in the papers [18,20,21,26,27]. These values are given only for SLM-samples of unalloyed titanium, which had high mechanical characteristics and high relative density of the material (more than 99%).

Finally, the obtained physical and mechanical characteristics of titanium VT1-0 can be represented as a generalized „SLM“ map in the coordinates „laser power–scanning speed“ (Fig. 7), which shows the areas of maximum values for a number of important physical and mechanical properties, such as density, strength and plasticity, and a single

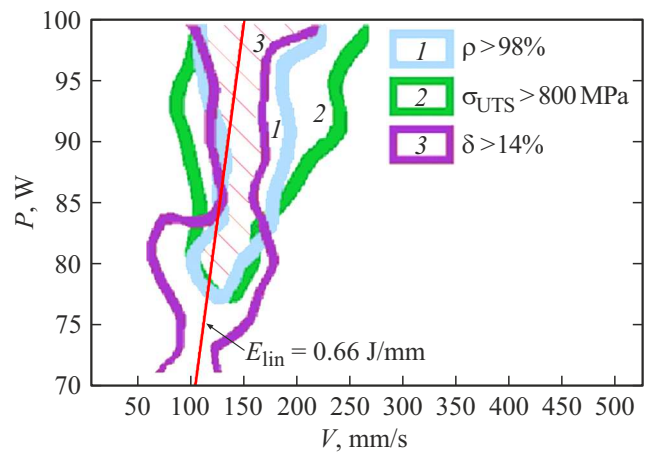


Figure 7. Regions of optimal SLM parameters for obtaining high characteristics of titanium VT1-0: 1 — relative density, 2 — ultimate tensile strength, 3 — elongation to failure.

area of parameters in which all these characteristics have maximum values simultaneously (shaded area). Titanium VT1-0, obtained in SLM-modes lying on a half-plane to the left and right of the optimal LED isoline 0.66 J/mm, has lower physical and mechanical characteristics compared to the material obtained at the optimal SLM parameters. At the same time, note that we assume that in other areas of the parameter plane „ laser power–scanning speed“, which are not studied in this paper (at powers above 100 W), the optimal SLM modes should also be identified for modes close to the LED isoline 0.66 J/mm.

Conclusion

Comprehensive studies of the physical and mechanical properties, and structure of samples of unalloyed titanium VT1-0, created by the SLM method, were carried out. In this paper the following is shown:

1. Under optimal SLM conditions high strength characteristics were obtained (ultimate tensile strength 820 MPa, yield strength 710 MPa), exceeding by 2 times the values for this material manufactured using conventional technologies.
2. The reason for the increase in the mechanical characteristics of titanium VT1-0 is the formation of a finely dispersed martensitic α' -phase, which is obtained due to the high crystallization rates realized in the SLM process.
3. It is shown that the SLM parameters significantly affect the structure and properties of the material. High mechanical characteristics are obtained at optimal values of the linear energy density 0.6–0.7 J/mm.

Funding

This study was supported by the Russian Science Foundation (grant № 22-19-00271).

Conflict of interest

The authors declare that they have no conflict of interest.

References

- [1] D.M. Brunette, P. Tengvall, M. Textor, P. Thomsen. *Titanium in Medicine: Material Science, Surface Science, Engineering, Biological Responses and Medical Applications* (Springer, Berlin, 2001)
- [2] A.T. Sidambe. *Materials*, **7**, 8168 (2014). DOI: 10.3390/ma7128168
- [3] N. Schiff, B. Grosogeat, M. Lissac, F. Dalard. *Biomaterials*, **23**, 1995 (2002). DOI: 10.1016/S0142-9612(01)00328-3
- [4] I.N. Friedlander. *Mashinostroenie. Entsiklopediya: Tsvetnye metally i splavy. Kompozitsionnye metallicheskie materialy* (Mashinostroenie, M., 2001), t. II-3. (in Russian)
- [5] *Implanty dlya khirurgii. Metallicheskie materialy. Implanty dlya khirurgii. Metallicheskie materialy. Chast 3. Deformiruemyj splav na osnove titana, 6-alyuminiya i 4-vanadiya* (GOST R ISO 5832-3-2020) (in Russian)
- [6] M. Geetha, A.K. Singh, R. Asokamani, A.K. Gogia. *Prog. Mater. Sci.*, **54**, 397 (2009). DOI: 10.1016/j.pmatsci.2008.06.004
- [7] J. Mazurek-Popczyk, L. Palka, K. Arkusz, B. Dalewski, K. Baldy-Chudzik. *Injury*, **53**, 938 (2022). DOI: 10.1016/j.injury.2021.12.020
- [8] A.X.Y. Guo, L. Cheng, S. Zhan, S. Zhang, W. Xiong, Z. Wang, G. Wang, S. C. Cao. *J. Mater. Sci. Technol.*, **125**, 252 (2022). DOI: 10.1016/j.jmst.2021.11.084
- [9] N.A. Koporushko, S.V. Mishinov, V.V. Stupak. *Politramma*, **3**, 54 (2020). (in Russian) DOI: 10.24411/1819-1495-2020-10033
- [10] S. Bo, S. Wen, C. Yan, Q. Wei, Y. Shi. *Selective Laser Melting for Metal and Metal Matrix Composites* (Academic Press, London, 2021), DOI: 10.1016/C2018-0-01940-4
- [11] I. Yadroitsev, I. Yadroitsava, A. Du Plessis, E. Macdonald. *Fundamentals of Laser Powder Bed Fusion of Metals* (Elsevier, 2021), DOI: 10.1016/C2020-0-01200-4
- [12] N.V. Kazantseva, P.V. Krakhmalev, I.A. Yadroitseva, I.A. Yadroitsev. *FMM* **122**, 8 (2021) (in Russian). DOI: 10.31857/S001532302101006X
- [13] F.N. Depboylu, E. Yasa, Ö. Poyraz, J. Minguella-Canela, F. Korkusuz, M.A. de los Santos López. *J. Mater. Res. Technol.*, **17**, 1408 (2022). DOI: 10.1016/j.jmrt.2022.01.087
- [14] H. Attar, M.J. Bermingham, S. Ehtemam-Haghighi, A. Dehghan-Manshadi, D. Kent, M.S. Dargusch. *Mater. Sci. Eng. A*, **760**, 339 (2019). DOI: 10.1016/j.msea.2019.06.024
- [15] C.-L. Li, C.-S. Wang, P.L. Narayana, J.-K. Hong, S.-W. Choi, J.H. Kim, S.W. Lee, C.H. Park, J.-T. Yeom, Q. Mei. *J. Mater. Res. Technol.*, **11**, 301 (2021). DOI: 10.1016/j.jmrt.2021.01.008
- [16] C.-L. Li, J.W. Won, S.-W. Choi, J.-H. Choe, S. Lee, C.H. Park, J.-T. Yeom, J.K. Hong. *J. Alloy Compd.*, **803**, 407 (2019). DOI: 10.1016/j.jallcom.2019.06.305
- [17] M.T. Hasib, H.E. Ostergaard, Q. Liu, X. Li, J.J. Kruzic. *Addit. Manuf.*, **45**, 102027 (2021). DOI: 10.1016/j.addma.2021.102027
- [18] H. Attar, S. Ehtemam-Haghighi, D. Kent, X. Wu, M.S. Dargusch. *Mater. Sci. Eng. A*, **705**, 385 (2017). DOI: 10.1016/j.msea.2017.08.103
- [19] L. Zhou, T. Yuan, J. Tang, J. He, R. Li. *Opt. Laser Technol.*, **119**, 105625 (2019). DOI: 10.1016/j.optlastec.2019.105625
- [20] B. Wysocki, P. Maj, A. Krawczyńska, K. Roźniatowski, J. Zdunek, K.J. Kurzydłowski, W. Świąszkowski. *J. Mater. Process. Tech.*, **241**, 13 (2017). DOI: 10.1016/j.jmatprotec.2016.10.022
- [21] D. Gu, Y.-C. Hagedorn, W. Meiners, G. Meng, R.J. Santos Batista, K. Wissenbach, R. Poprawe. *Acta Mater.*, **60**, 3849 (2012). DOI: 10.1016/j.actamat.2012.04.006
- [22] D. Herzog, V. Seyda, E. Wycisk, C. Emmelmann. *Acta Mater.*, **117**, 371 (2016). DOI: 10.1016/j.actamat.2016.07.019
- [23] H.D. Nguyen, A. Pramanik, A.K. Basak, Y. Dong, C. Prakash, S. Debnath, S. Shankar, I.S. Jawahir, S. Dixit, D. Buddhi. *J. Mater. Res. Technol.*, **18**, 4641 (2022). DOI: 10.1016/j.jmrt.2022.04.055
- [24] A. Atae, Y. Li, M. Brandt, C. Wen. *Acta Mater.*, **158**, 354 (2018). DOI: 10.1016/j.actamat.2018.08.005
- [25] H. Attar, M. Calin, L.C. Zhang, S. Scudino, J. Eckert. *Mater. Sci. Eng. A*, **593**, 170 (2014). DOI: 10.1016/j.msea.2013.11.038
- [26] Q. Tao, Z. Wang, G. Chen, W.C.P. Cao, C. Zhang, W. Ding, X. Lu, T. Luo, X. Qu, M. Qin. *Addit. Manuf.*, **34**, 101198 (2020). DOI: 10.1016/j.addma.2020.101198
- [27] Y.P. Dong, J.C. Tang, D.W. Wang, N. Wang, Z.D. He, J. Li, D.P. Zhao, M. Yan. *Mater. Design*, **196**, 109142 (2020). DOI: 10.1016/j.matdes.2020.109142
- [28] T. Mishurova, K. Artzt, J. Haubrich, G. Requena, G. Bruno. *Addit. Manuf.*, **25**, 325 (2019). DOI: 10.1016/j.addma.2018.11.023
- [29] P. Tan, R. Kiran, K. Zhou. *J. Manuf. Process.*, **64**, 816 (2021). DOI: 10.1016/j.jmapro.2021.01.058
- [30] H. Wang, Y. Zou. *Int. J. Heat Mass Tran.*, **142**, 118473 (2019). DOI: 10.1016/j.ijheatmasstransfer.2019.118473
- [31] H. Salem, L.N. Carter, M.M. Attallah, H.G. Salem. *Mater. Sci. Eng. A*, **767**, 138387 (2019). DOI: 10.1016/j.msea.2019.138387